Journal of Mammalogy, XX(X):1–12, 2020
DOI:10.1093/jmammal/gyz214

Morphometric analysis of skull shape reveals unprecedented diversity of African Canidae

Fabio Andrade Machado* and Pablo Teta

Department of Biology, University of Massachusetts, 100 William T. Morrissey Blvd, 02125-3393, Boston, USA (FAM)
División Mastozoología, Museo Argentino de Ciencias Naturales "Bernardino Rivadavia"-CONICET. Av. Ángel Gallardo 470 (C1405DJR), Buenos Aires, Argentina (FAM, PT)

**Correspondent: macfabio@gmail.com*

We conducted a geometric morphometric analysis to investigate the morphological variation of the golden wolf, *Canis lupaster*, and to clarify the morphological and taxonomic affinities of different taxa of the genera *Canis* and *Lupulella*. We suggest that the variation observed within the complex of *Canis lupaster* may be incompatible with what would be expected for a single species. We hypothesize that the nominal form *C. l. soudanicus* is a synonym of *Lupulella adusta* instead of being part of the golden wolf complex. The subspecies *C. l. bea* has a generalized jackal morphology (i.e., clusters together with *L. mesomelas* and *C. aureus*) and *C. l. lupaster* occupies an intermediate morphospace position, between jackal-like forms and wolf-like forms. These results contrast with previously published molecular analysis in which mitochondrial data failed to identify differences between golden wolf populations, and nuclear evidence points to the existence of groups that are incompatible with those recovered by morphological analysis. Regarding other jackals, our results depict the absence of morphological overlap between *L. m. mesomelas* and *L. m. schmidti* and no differences between putative subspecies of *L. adusta*. We call attention to the need for more integrative approaches to solve the taxonomic situation of various African Canidae.

Key words: *Canis anthus*, *Canis aureus*, *Canis lupus*, geometric morphometric, linear discriminant analysis, taxonomy

The golden wolf, a species for which both the names *Canis anthus* F. Cuvier, 1820 and *C. lupaster* Hemprich and Ehrenberg, 1833 were used, is a recently revalidated member of the genus *Canis*, a group that includes dogs, wolves, jackals, and coyotes (Viranta et al. 2017). Records of this species probably go back to the Greek geographer and historian Herodotus (484–425 B.C.), who noticed that wolves from Egypt were only slightly larger than foxes. Given that Herodotus was most likely familiar with both the Eurasian golden jackal, *C. aureus* Linnaeus, 1758, and the gray wolf, *C.* cf *lupus* Linnaeus, 1758, this not only suggested the presence of wolves in Africa, but also that the wolf species present there were somehow distinct from the ones found throughout Eurasia (Gaisford 1824). Remarks about the similarity between the golden wolf and the gray wolf can also be found in the works of Aristotle (384–322 B.C.), who associated the smaller size of the African wolf, in comparison to the Greek wolf, with the lower availability of food. Despite being classically recognized as a wolf-like species (Hemprich and Ehrenberg 1831), many authors have recurrently described African golden wolf populations as belonging to the same species as the Eurasian golden jackal, a classification that endured throughout most of the last century (Moehlman and Hayssen 2018). Besides this, many authors have noticed the resemblance of the golden wolves with gray wolves, specifically those from the Middle East and India (Ferguson 1981), further confusing the taxonomic status of this African canid.

The advent of modern molecular investigations showed that the golden wolf was not only more closely related to gray wolves than to Eurasian golden jackals (Rueness et al. 2011; Gaubert et al. 2012), but that it warranted full specific status (Koepfli et al. 2015). Currently, all African populations previously assigned to *C. aureus* are associated with the golden wolf, a species that is considered closely related to gray wolves and coyotes (*C.* cf *lupus* and *C. latrans*, respectively—Gaubert et al. 2012; Koepfli et al. 2015; Urios et al. 2015; Viranta et al. 2017; Gopalakrishnan et al. 2018). Despite being initially recognized under the name *C. anthus* by Koepfli et al. (2015), Viranta et al.

(2017) noticed that the original type described by Cuvier was lost, and that the descriptions provided by him alone were not sufficient to discriminate the type from other sympatric canid species, such as the side-striped jackal, *L. adustus* (Sundevall 1847). Thus, these authors considered *anthus* F. Cuvier, 1820 a *nomem dubium* and proposed the use of the name *C. lupaster* for the African golden wolf. The name *C. lupaster* has also been used to refer to the Egyptian population due to its morphological distinctiveness, setting it aside from the remaining African populations that were referred as *C. anthus* (Saleh and Basuony 2014).

As currently recognized, *C. lupaster* is thought to be a highly morphologically variable species (Bertè 2017; Viranta et al. 2017; Saleh et al. 2018). This is evident from the recurrent description of many morphotypes, usually two, throughout its distribution. Besides the aforementioned Egyptian population (*C. l. lupaster*), which is considered to be larger than other African jackal or wolf populations, smaller morphs are described from both western and southern portions of its distribution (Van Valkenburgh and Wayne 1994; Saleh and Basuony 2014). Gaubert et al. (2012) provided photographic evidence of the presence of two morphs at a single locality in Senegal, suggesting that part of the variability of this species is not geographically structured. Morphometric analyses by Viranta et al. (2017) are consistent with this hypothesis, as these authors found that geographically defined groups were more variable than the Eurasian populations of the golden jackal, *C. aureus*. This could be because *C. lupaster* refers to more than one species, one being the small morph and another the large morph. This distinction has been proposed in the past by De Beaux (1923), who referred to the larger morph as *C. lupaster* and the smaller one as *C. anthus.* This designation has been used recently by some authors (Bertè 2017; Saleh et al. 2018).

Analysis of mitochondrial DNA, however, failed to find clear structure between these two morphs (Gaubert et al. 2012; Koepfli et al. 2015; Viranta et al. 2017; Gopalakrishnan et al. 2018; Saleh et al. 2018), suggesting that all African populations derive from the same stock. A recent nuclear genome-wide analysis (Gopalakrishnan et al. 2018) showed that the golden wolf originated from a hybridization event between the gray wolf and the Ethiopian wolf, *C. simensis* Rüppell, 1840 (or some closely related extinct species). Different degrees of gene flow among these species helped to establish genetic differences between northwestern (Algeria, Morocco, Senegal) and eastern (Ethiopia, Kenya) populations of the golden wolf. A similar population structure was found in a microsatellite analysis done by Koepfli et al. (2015), who reported that the population from Kenya differed from those of the northwest of the continent (Algeria, Morocco, Mauritania, Senegal). Unfortunately, Koepfli et al. (2015) did not sample any individual from Egypt, and the only specimen from the Egyptian population sampled by Gopalakrishnan et al. (2018) represented a dog-golden wolf hybrid, impeding any assessment of this highly morphologically distinct population.

The possibility of hybridization presents a challenge for canid taxonomy. Many wild species naturally hybridize (e.g., Khosravi et al. 2013; Way 2013; Pilot et al 2018), with some populations and species being hypothesized to be of hybrid origin, such as is the case of the North American red wolf, *C. rufus* Audubon and Bachman, 1851, and the great lakes wolf, *C. lycaon* Schreber, 1775 (vonHoldt et al. 2016). Evidence of the importance of introgression in the origin of Canidae species is accumulating (Gopalakrishnan et al. 2018), raising the possibility of recent hybridization as a cause of morphological novelties and species formation (Marques et al. 2019).

While morphometric analyses of the golden wolf have had a wide geographical coverage (Van Valkenburgh and Wayne 1994; Bertè 2017), they usually are limited in terms of taxonomic scope. These studies tend to compare golden wolves with either the gray wolf (*C.* cf. *lupus*—Ferguson 1981; Bertè 2017) or the European golden jackal (*C. aureus*—Koepfli et al. 2015), but rarely both, and usually neglect other African jackals, such as the side-striped jackal, *Lupulella adusta* (Sundevall 1847), and the black-backed jackal, *L. mesomelas* (Schreber 1775) (see Supplementary Data provided by Viranta et al. 2017 for a rare exception). Here, we investigate the morphological variation of the golden wolf in a broader taxonomic context to clarify the morphological and taxonomic affinities of different groups. We investigate the craniometric variation of the species using geometric morphometrics on a large sample, covering key taxa that have either been historically associated with the golden wolf or that overlap geographically and morphologically with this species.

Materials and Methods

Sample.—We investigated 301 skulls of Canidae housed at the following institutions: Museu de Zoologia da Universidade de São Paulo (MZUSP, São Paulo), Museu Nacional (MN, Rio de Janeiro), Museum of Vertebrate Zoology (MVZ, Berkeley), American Museum of Natural History (AMNH, New York), National Museum of Natural History of the Smithsonian Institution (USNM, Washington), Museum of Comparative Zoology (MCZ, Harvard), Field Museum (FMNH, Chicago), and Academy of Natural Sciences of Drexel University (ANSP, Philadelphia). We only evaluated specimens with teeth fully erupted and closed sutures to limit ontogenetic variation.

We focused our sampling on African and south Asian members of the genera *Lupulella* and *Canis* that have been historically associated with the golden wolf (Fig. 1), such as the golden jackal (*C. aureus*) and the Indian wolf (*C.* cf. *l. pallipes* Sykes, 1831). Because of the genetic similarities between the golden wolf and the Himalayan wolf (*C.* cf. *l. chanco* Gray, 1863), specimens from this taxon were also included. Lastly, because *C.* cf. *l. pallipes* and *C.* cf. *l. chanco* are thought to be early divergent lineages of *C.* cf. *lupus*, we included a wide North American sample of *C.* cf *lupus* as a baseline comparison for the species. Here, we chose the designation of *Lupulella* for both side-striped (*L. adusta*) and black-backed jackals (*L. mesomelas*) following Viranta et al. (2017—see discussion on their Additional file 1) and due to results of recent total-evidence cladistic analysis of canids, which recovered both

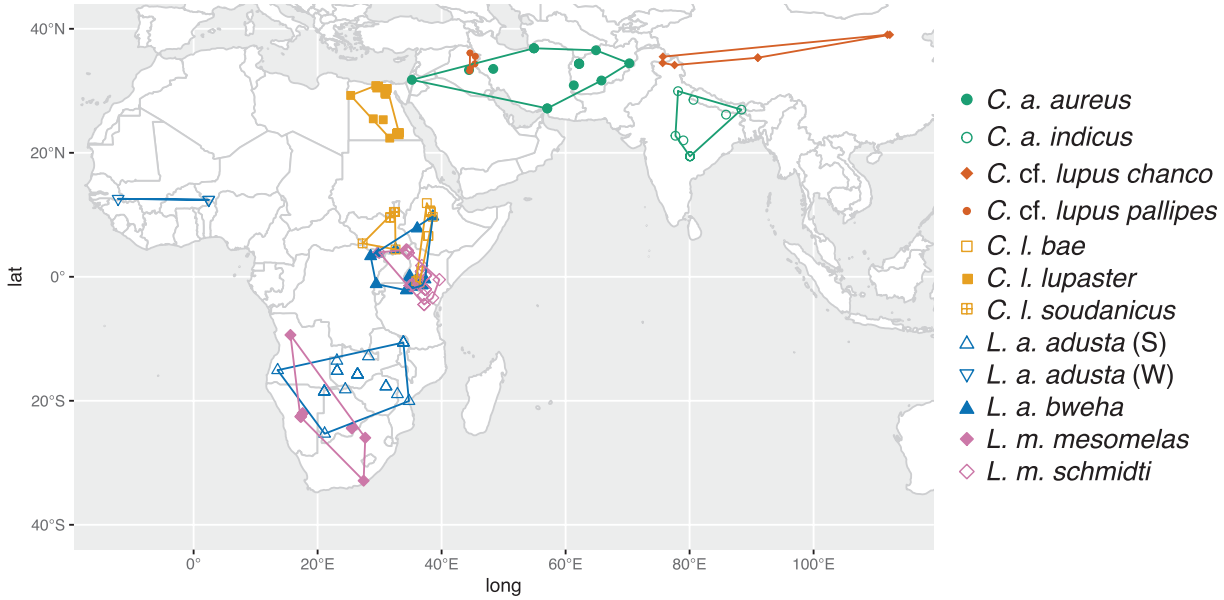

Fig. 1.—Map depicting the distribution of African and Asian samples of *Canis* and *Lupulella* subspecies analysed in the present study.

species to be sister to each other (Zrzavy et al. 2018; but see Atickem et al. 2017 for a discussion on the possibility of both species belonging to a different genus).

Within each species, individuals were assigned to subspecies based on their geographical location, following the described subspecies distributions (Fig. 1; Mech 1974; Walton and Joly 2003; Sillero-Zubiri et al. 2004; Moehlman and Hayssen 2018). The only exceptions to this rule were *L. adusta*, in which one subspecies was further divided due to its ample geographical distribution, and *C.* cf. *lupus*, in which North American samples were pooled according to their overall morphological similarity (see below).

Nevertheless, we henceforth refer to these groups as "subspecies" for simplicity. For *L. adusta*, we sampled two broadly distributed subspecies: *L. a. adusta* and *L. a. bweha* Heller, 1914, with the first being further divided into two populations, referent to extremes of its distribution to the west and the south of the continent (*L. a. adusta* (W) and *L. a. adusta* (S), respectively). *Lupulella mesomelas* was divided into two geographically disjoint populations that are currently recognized as two distinct subspecies: *L. m. mesomelas* to the south and *L. m. schmidti* (Noack, 1897) to the east. For *C. lupaster*, we sampled three subspecies, *C. l. bea* (Heller, 1914) to the eastern portion of the continent, *C. l. lupaster* from northern Egypt, and *C. l. soudanicus* Thomas, 1903 for the Sudan. *Canis aureus* was divided into two subspecies: *C. a. aureus*, from the Middle-East region and *C. a. indicus* Hodgson, 1833 from India. *Canis* cf. *lupus* was divided into four groups: Himalayan wolves (*C.* cf. *l. chanco*), Indian wolves (*C.* cf. *l. pallipes*), wolves from northern North America (*C.* cf. *lupus* NNA), and wolves from southern North America (*C.* cf. *lupus* SNA). North American *C.* cf. *lupus* were divided in this way because a preliminary inspection of these groups did not reveal any clear pattern according to traditionally recognized subspecies. Table 1 shows the total sample discriminated by species, group, and sex, as well as the geographical origin of the samples.

Table 1.—Sample sizes of the members of African, Asian, and North-American *Canis* and *Lupulella* analysed in the present study. [a] Group: W, West; E, East; NNA, Northern North America; SNA, Southern North America. [b] Sex: F, female; M, male; U, unknown.

Taxon	Group[a]	Sex[b]		
		F	M	U
Lupulella				
L. adusta	*L. a. adustus* (E)	10	8	
	L. a. adustus (W)	0	3	
	L. a. bweha	10	10	
L. mesomelas	*L. m. mesomelas*	6	6	1
	L. m. schmidti	19	23	1
Canis				
C. lupaster	*C. l. bea*	9	7	
	C. l. lupaster	15	21	1
	C. l. soudanicus	5	2	
C. aureus	*C.a.aureus*	9	7	
	C.a.indicus	5	4	
C. lupus	*C.* cf. *l. chanco*	3	4	1
	C. cf. *l. pallipes*	3	1	1
	*C.*cf. *lupus* (NNA)	38	48	
	*C.*cf. *lupus* (SNA)	6	14	
	Total =	301		

Geometric morphometrics.—A total of 43 anatomical landmarks (9 on the midline and 17 on each side of the skull; Fig. 2) were digitized using a Microscribe MLX system. Each skull was digitized twice and the average (after translation and rotation, but not scaling—Schönemann 1966) was taken as the shape of the individual. Additionaly, we removed the asymmetric variation of the shapes following Klingenberg et al. (2002) to obtain only symmetric shapes. The resulting full sample was submitted to a generalized Procrustes analysis (GPA—Rohlf and Slice 1990) with the package Morpho (Schlager 2017), and the superimposed configurations were then projected on a tangent

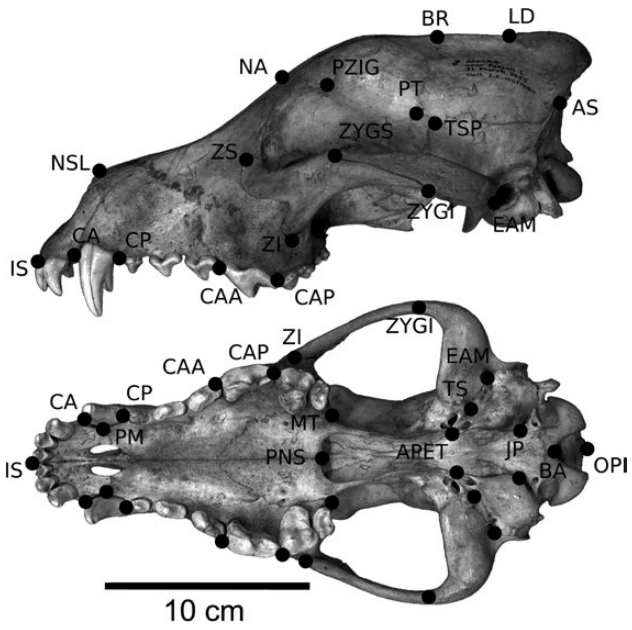

Fig. 2.—Landmarks used, represented on a *Canis lupus* skull. Landmarks modified from Machado et al. (2018, 2019).

Euclidian space to allow for standard statistical procedures (Slice 2001). The covariance matrix of Procrustes residuals (the difference between the mean shape and observed shapes) was subjected to a principal component analysis (PCA) for data visualization and dimensionality reduction.

Initially, we performed a two-way analysis of covariance to evaluate if there are any differences among species and sexes. An interaction term was added to evaluate if sexual dimorphism was consistent within the sample. Also, the log-centroid size was added as a covariate to account for changes due to allometric variation. This was done using the function procD.lm of the package geomorph (Adams et al. 2019), which uses permutations to evaluate if different factors have a significant effect on shape. Effects sizes were calculated using a *z*-score approach that allows for their direct comparison among different kinds of factors.

To evaluate if the morphological variation observed within the golden wolf groups is consistent with what is observed for other species, we calculated the within-group disparity and compared them among taxa. As a measure of disparity, we calculated the squared Mahalanobis distance between each individual and its group mean as $D_i^2 = (x_i - \acute{x})^T W^{-1} (x_i - \acute{x})$, where x_i is the vector of multivariate phenotype of the individual i, x^i is the average of the species and W^{-1} is the inverse of the pooled within-group covariance matrix obtained for the entire sample. The squared Mahalanobis distance takes into account the patterns of shape covariation and is given in units of variance, thus being a good estimate of within-group shape divergence. To evaluate if any group showed more variation than others, we performed pairwise *t*-tests for differences in Mahalanobis distances between all groups, with *P*-values being corrected for multiple tests using Bonferroni adjustment. This analysis was performed on both the species and subspecies levels.

To evaluate differences among subspecies, we performed a linear discriminant analysis (LDA) as implemented in Morpho (Schlager 2017), which performs two main operations. First, it calculates a new set of axes of variation that maximizes discrimination among groups (Campbell and Atchley 1981). Shape changes along those new axes can be visualized by back-transforming extreme scores along each axis onto the shape space. Second, it calculates the pairwise Mahalanobis distance among group averages and confronts it with a null distribution produced by permuting group identity among observations. This is equivalent to a non-parametric multivariate analysis of variance (np-MANOVA) performed on Mahalanobis distances (Anderson 2001). Additionally, we performed a leave-one-out cross-validation (CV) analysis to assess the reliability of the a priori group classifications, and group superposition (Machado and Hingst-Zaher 2009). This analysis consists of removing each individual from the sample and recalculating the LDA. The removed individual is then projected on the new LDA space and is assigned to the group with the closest group average (Mitteroecker and Bookstein 2011).

Lastly, we evaluated the role of allometric size differences in driving between-group differentiation. To visualize shape changes associated with intraspecific allometric variation, we calculated the common allometric component (CAC—Mitteroecker et al. 2004), using the subspecies as groupings. The CAC axis was then compared with LD axes by calculating the Pearson's product–moment correlation coefficient among CAC and LD scores. Furthermore, shape changes associated with CAC and LD axes were directly compared through vector correlation.

Results

The two-way analysis of covariance of shape showed that, even though size was significantly associated with shape, group differences were still significant after accounting for allometric variation (Table 2). The analysis also identified the presence of sexual dimorphism in the sample, both as a direct effect of sex and as the interaction between subspecies and sex (species-specific sexual dimorphism). Standardized *z*-scores show that the main effect size is associated with shape differences among groups, followed by allometric shape changes. Both sex and interaction between subspecies and sex had small effect sizes when compared to the other factors (Table 2). Analysis of individual sexes showed the same general patterns and led to the same conclusions as the one performed on the full sample. For simplicity, all results shown here are based on the analyses of both sexes pooled, including individuals of unknown sex (Table 1).

The first two PCs of the PCA of superimposed Procrustes residuals represent the main patterns of shape variation (44.94% of the total variation) and are used to illustrate groups' disparity (Fig. 3). PC1 contrasts African jackals (*L. adusta*, *L. mesomelas*, and *C. lupaster* except for *C. l. lupaster*) with negative values and *C. lupus* with positive values, and represents an overall distinction between gracile (negative values)

and robust (positive values) forms. PC2 contrasts *L. m. schmidti* with negative values and *L. adusta* with positive values, and distinguishes forms with shorter (negative values) and longer (positive values) snouts. On the morphospace defined by these two PCs, *C. lupaster* shows intermediate values on average, but overlaps with all other species, suggesting greater shape variation within this group than in other taxa.

The comparison between intraspecific squared Mahalanobis distance (D^2) is consistent with this interpretation, as *C. lupaster* stood out as the group with most disparity (Fig. 4A). Furthermore, pairwise *t*-tests revealed that the disparity observed for *C. lupaster* was the only one that was significantly different from other groups (Fig. 4A; Supplementary Data SD1). Inspection of D^2 for subspecies revealed intragroup disparities that were not only smaller than the ones observed for the species-level analysis, but that was also consistent among all subspecies (Fig. 4B). Despite this, some subspecies presented disparities that were slightly higher than others, such as *C.* cf. *l. chanco* and *C.* cf. *lupus* (SNA). However, the only comparisons that were significant were those performed against subspecies with the lowest disparities, such as *L. m. mesomelas*, *L. m. schmidti*, and *C. a. aureus* (in the case of *C.* cf. *l. chanco*), and of *C.* cf. *lupus* (NNA; in the case of *C.* cf. *lupus* [SNA]; Supplementary Data SD2).

The inspection of the two first axes of the LDA revealed a similar pattern to the one found in the PCA, with the LD1 discriminating *C.* cf *lupus* taxa from other taxa, and LD2 mostly discriminating *L. adusta* from others (Fig. 5). The shape deformations associated with these axes were nearly identical to the ones seen for PCA, with LD1 showing a vector correlation of 0.99 with PC1, and LD2 showing a vector correlation of 0.95 with PC2. For this reason, shape representations were omitted for simplicity. The dispersion of subspecies shows that while most subspecies tend to be similar to other groups from the same species, this is not the case for *C. lupaster*. While *C. l. bea* falls somewhere between *L. mesomelas* and *C. aureus*, *C. l. soudanicus* groups with *L. adusta*, and *C. l. lupaster* falls between *C. lupus* and the remaining jackal populations. While there is a slight overlap between *C. l. bea* and *C. l. lupaster*, *C. l. soudanicus* do not overlap with either of the former golden wolf subspecies.

The permutation analysis of Mahalanobis distance between groups revealed that, while most pairwise differences are significant (Table 3), some exceptions are evident. Specifically, both golden jackal subspecies *C. a. indicus* and *C. a. aureus* were indistinguishable from each other, as well as both Asian gray wolf taxa analyzed, *C.* cf. *l. chanco* and *C.* cf. *l. pallipes*. Within the gray wolf complex, the test was unable to discriminate *C.* cf. *lupus* (SNA) from both *C.* cf. *l. chanco* and *C.* cf. *l. pallipes*. Within African taxa, three subspecies could not be distinguished from each other: both subspecies of the side-striped jackal, *L. a. adusta* (S) and *L. a. adusta* (W), and the golden wolf from Sudan, *C. l. soudanicus*.

The results from the leave-one-out cross-validation (CV) analysis are broadly concordant with those of the permutation analysis (Table 4). CV shows that there is a large morphological overlap between all *L. adusta* subspecies, not only with each other but also with *C. l. soudanicus*. *Canis aureus* showed high misclassification rates among subspecies, suggesting high morphological similarity among geographical groups. Similarly, *C.* cf. *lupus* showed a high morphological overlap among different subspecies, with the North American group being the most distinctive. *Lupulella mesomelas*, on the other hand, showed high correct classification rates at the subspecies level, suggesting little morphological overlap among groups. Lastly, minor overlaps (1 individual) exist between *C. l. lupaster* and *C.* cf. *l. chanco*, *C. a. indicus* and *C. l. bea*, and *C. l. lupaster* and *C. l. bea*.

Analysis of covariance showed that, while there is significant size-related shape change in the sample, allometric variation is unable to explain all variation (Table 2). Furthermore, effects sizes related to allometric scaling were considerably lower than the ones for between-groups differences, suggesting that groups are more different than expected only due to allometric scaling. The common allometric component (CAC) analysis shows that size-related shape changes are mostly concentrated on the braincase region, and represent a contrast between small individuals with relatively larger braincases and larger individuals with relatively small braincases (Fig. 6). While Pearson's correlation among LD1 and CAC scores were high (cor = 0.977, $P < 2.2e\text{-}16$), vector correlation was moderate (cor = 0.551). Correlations between CAC and other LD vectors were not considered significant on Pearson's correlation analysis ($P > 0.05$) and presented low vector correlation values (cor ≤ 0.296). Other visualizations of allometric changes that take into account differences of slope (e.g., plotAllometry function of package geomorph—Adams et al. 2019) have revealed similar patterns.

Discussion

Species delimitation in canids has always been a challenge. According to the biological species concept, species should be

Table 2.—Multivariate two-way analysis of covariance of skull shape variation in Canidae, evaluating the effect of geographical groups (subspecies of *Canis* and *Lupulella*) and sex, taking log(CS) (size) as a covariate. *d.f.* = degrees of freedom of the factors; SS = sum of squares; MS = mean squares; R^2 = coefficient of determination; *F* = approximate *F*-statistic; *Z* = *z*-standardized effect size. Pr(>*F*) = *P*-value.

	d.f.	SS	MS	R^2	*F*	*Z*	Pr(>*F*)
log(CS)	1	0.012	0.012	0.018	10.614	7.422	1.00E-04
Subspecies	13	0.171	0.013	0.243	11.321	20.630	1.00E-04
Sex	1	0.002	0.002	0.003	1.760	1.949	0.026
Subspecies:Sex	12	0.017	0.001	0.024	1.209	1.966	0.025
Residuals	268	0.311	0.001	0.443			
Total	295	0.702					

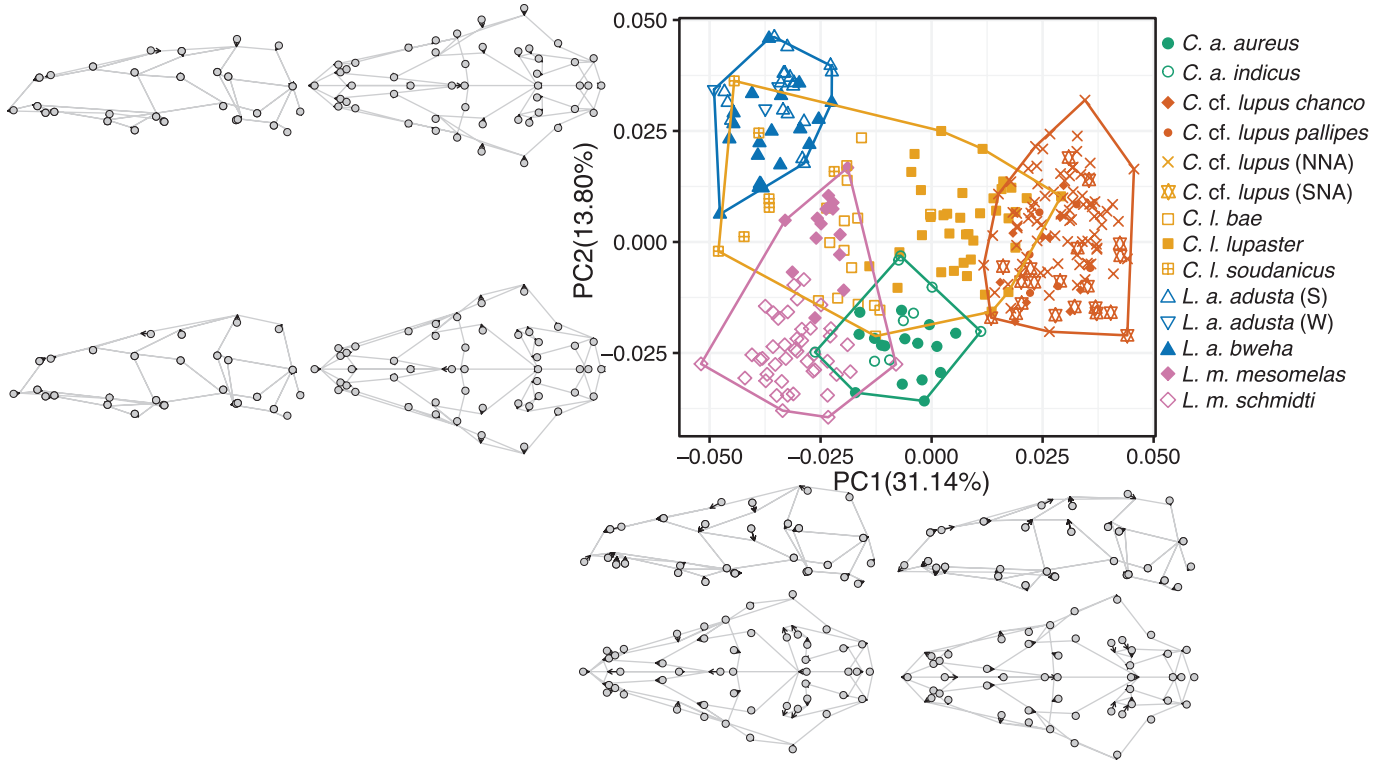

Fig. 3.—Principal component analysis of skull shape variation of African, Asian, and North-American members of *Canis* and *Lupulella* species. Different colors represent different species and different shapes represent different subspecies. Polygons are minimum convex hulls for each species. Configurations represent shape changes along each axis on both lateral and dorsal views. Shape changes are displayed as a difference between the mean shape and three standard deviations away from the mean on both positive and negative extremes of the axis.

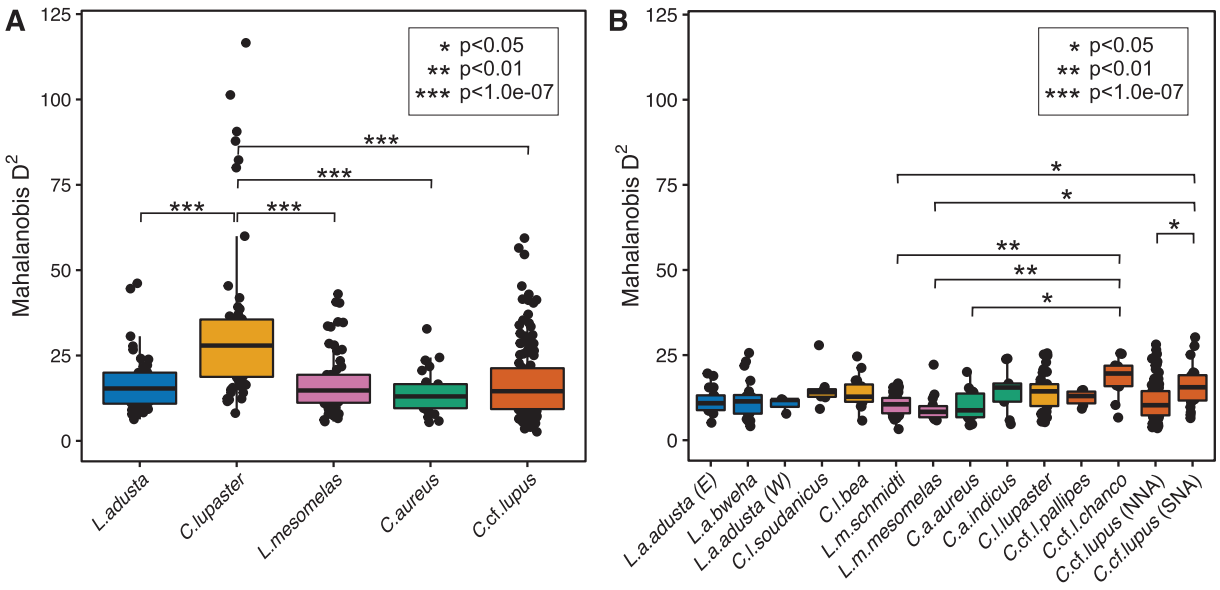

Fig. 4.—Skull shape disparity within each species (A) and subspecies (B) of *Canis* and *Lupulella* measured as squared Mahalanobis distance between each observation and the group mean. Asterisks refer to significant *P*-values (<0.05) of *t*-tests on the differences in averages corrected for multiple comparisons.

composed of individuals that are unable to interbreed with individuals from other species (Mayr 1942). However, it has long been recognized that members of the genus *Canis* readably hybridize in the wild, and that some of those hybrids are viable and might be able to form hybrid taxa that are ecologically and morphologically distinct from their parent species (vonHoldt

et al. 2016; Hohenlohe et al. 2017; Heppenheimer et al. 2018). Furthermore, identification of taxa based on cranial or external morphology alone can be challenging, as recently divergent taxa might differ in very subtle ways (Prevosti et al. 2013; Chemisquy et al. 2019). While morphological similarity might not be indicative of conspecificity, the existence of discrete morphological discontinuities remains as a common signal for distinct species (Gaubert and Antunes 2005; Diersing and Wilson 2017). Thus, even when morphology might fail to find evidence of species differentiation, morphological diagnosability is often indicative of species separation (e.g., Miranda et al. 2017).

Our morphometric analysis of the *Canis lupaster* complex (referred hereafter as the "golden wolf complex") suggests that the variation observed within this group may be incompatible with what would be expected for a single *Canis* species. This is made clear in the analysis of morphological disparity, in which the disparity within the golden wolf complex as a whole is larger than that observed for any other species (Fig. 4A). This could mean that the golden wolf is an unusually variable species, as has been previously suggested (Viranta et al. 2017). However, the disparity observed within this taxon is even greater than the one observed for the gray wolf (Figs. 3 and 4A), a taxon that is widely distributed across three continents, with a large variety of forms (Pocock 1935), and that probably refers to an ensemble of species (Chetri et al. 2016; Heppenheimer et al. 2018). Furthermore, the variation within the golden wolf complex is nearly discrete, in stark contrast to the variation in the gray wolf complex, which presents large overlaps even between distantly related lineages, such as southern North American and Indian wolves (Figs. 3, 5, and 6). Nonetheless, when the sample is partitioned into subspecies, disparity observed for *C. lupaster* subspecies falls well within the range for other groups (Fig. 4B). These results suggest that the increased disparity observed for the golden wolf complex is probably an artifact of the pooling of morphologically heterogeneous groups, here represented by subspecies, under the same species label.

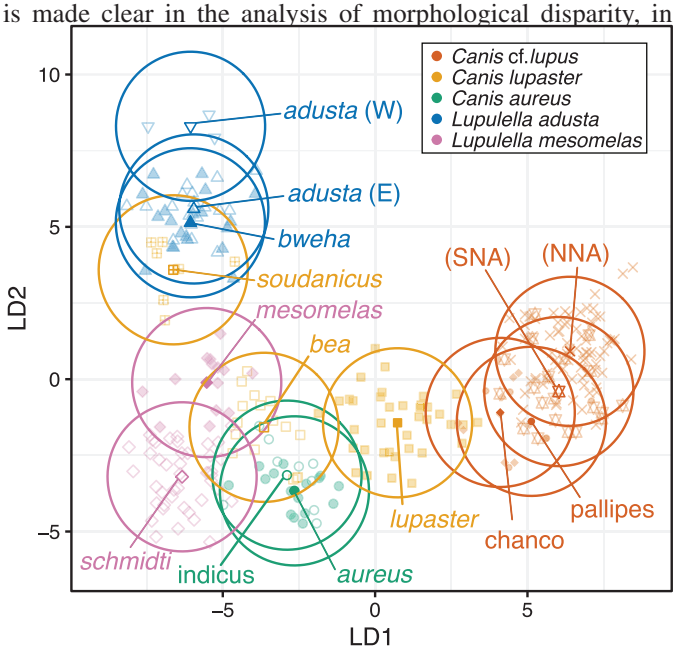

Fig. 5.—Distribution of individuals and subspecies averages on the first two axes of the linear discriminant analysis of skull shape variation of members of *Canis* and *Lupulella*. Circles represent the 95% confidence intervals based on the pooled within-group covariance of the a priori defined groups.

The first one of these groups is *C. l. soudanicus*, a small subspecies supposedly endemic from Sudan. Not only is *C. l. soudanicus* distinct from the remaining subspecies of *C. lupaster*, but it also largely overlaps with samples from different populations of *L. adusta* (Fig. 5). While convergence could be an explanation, a qualitative evaluation of the morphology of their skull shows little difference between these taxa other than size (Supplementary Data SD3), suggesting that *C. l. soudanicus* might be a synonym of *L. adusta*. This is particularly puzzling given that both *C. l. soudanicus* and *L. a. bweha* have been recognized as different taxa by Setzer (1956) in his review of the mammals of Sudan. The recognition of two species instead of one could be partially explained by size differences between the putative groups, as *C. l. soudanicus* had the smallest skull size of the whole sample (Fig. 6). Allometric scaling can lead to substantial morphological differences in Canidae (Wayne 1986; Morey 1992; Machado et al 2018), helping to explain why these groups were classically identified as distinct, even in sympatry (e.g., Voss et al. 2014). This idea

Table 3.—Permutation analysis of Mahalanobis distance among *Canis* and *Lupulella* subspecies mean shapes. Values below the diagonal are the Mahalanobis distance among group means and values above it are *P*-values obtained from 10,000 permutations.

	1	2	3	4	5	6	7	8	9	10	11	12	13	14
1. *C. a. aureus*		0.6795	**0.0001**	**0.0001**	**0.0001**	**0.0001**	**0.0001**	**0.0001**	**0.0001**	**0.0001**	**0.0001**	**0.0001**	**0.0001**	**0.0001**
2. *C. a. indicus*	3.076		**0.0004**	**0.0003**	**0.0001**	**0.0001**	**0.0123**	**0.0090**	**0.0013**	**0.0001**	**0.0001**	**0.0001**	**0.0023**	**0.0009**
3. *C.* cf. *l chanco*	9.736	8.937		0.2486	**0.0164**	0.0760	**0.0001**	**0.0019**	**0.0001**	**0.0001**	**0.0001**	**0.0001**	**0.0001**	**0.0001**
4. *C.* cf. *l pallipes*	10.955	10.264	5.043		**0.0448**	0.1773	**0.0002**	**0.0018**	**0.0001**	**0.0001**	**0.0001**	**0.0001**	**0.0001**	**0.0001**
5. *C.* cf. *lupus* (NNA)	11.547	10.850	4.973	5.519		**0.0164**	**0.0001**	**0.0001**	**0.0001**	**0.0001**	**0.0001**	**0.0001**	**0.0001**	**0.0001**
6. *C.* cf. *lupus* (SNA)	11.371	10.608	4.700	4.893	3.744		**0.0001**	**0.0001**	**0.0001**	**0.0001**	**0.0001**	**0.0001**	**0.0001**	**0.0001**
7. *C. l. bea*	8.135	6.283	9.821	10.687	11.523	11.455		**0.0001**	**0.0004**	**0.0001**	**0.0001**	**0.0001**	**0.0105**	**0.0001**
8. *C. l. lupaster*	7.224	5.714	6.342	7.728	7.299	7.617	6.853		**0.0001**	**0.0001**	**0.0001**	**0.0001**	**0.0001**	**0.0001**
9. *C. l. soudanicus*	10.018	9.059	12.394	13.883	13.949	14.086	8.826	10.713		0.0624	0.1300	0.1804	**0.0071**	**0.0001**
10. *L. a. adusta* (S)	11.111	9.95	12.739	13.931	13.44	13.945	9.415	10.38	5.585		0.2209	0.1549	**0.0002**	**0.0001**
11. *L. a. adusta* (W)	14.37	13.259	14.814	16.162	15.216	15.588	12.153	13.336	7.671	6.294		0.2947	**0.0019**	**0.0001**
12. *L. a. bweha*	10.575	9.449	12.718	13.955	13.322	13.743	8.904	10.164	4.547	3.483	5.841		**0.0004**	**0.0001**
13. *L. m. mesomelas*	9.556	7.587	10.956	12.083	12.714	12.743	5.738	8.117	7.547	7.444	10.658	7.581		**0.0005**
14. *L. m. schmidti*	8.221	6.815	11.587	12.745	13.605	13.12	7.381	9.31	8.532	9.637	12.509	9.12	6.123	

Table 4.—Classification rates based on the cross-validation analysis of shape variables among subspecies *Canis* and *Lupulella*. Rows are the a priori group assignments and columns represent the a posteriori group assignments. The diagonal contains the correct classification rates for each group.

	1	2	3	4	5	6	7	8	9	10	11	12	13	14
1. *C. a. aureus*	81.25	18.75												
2. *C. a. indicus*	55.56	33.33					11.11							
3. *C.* cf. *l chanco*			50.00	20.00	20.00			10.00						
4. *C.* cf. *l pallipes*			16.67	50.00		33.33								
5. *C.* cf. *lupus* (NNA)					96.51	3.49								
6. *C.* cf. *lupus* (SNA)			5.00		20.00	75.00								
7. *C. l. bea*							100.00							
8. *C. l. lupaster*							2.70	97.30						
9. *C. l. soudanicus*									57.14	14.29		28.57		
10. *L. a. adusta* (S)										83.33		16.67		
11. *L. a. adusta* (W)											66.67	33.33		
12. *L. a. bweha*									10.00	20.00		70.00		
13. *L. m. mesomelas*													100.00	
14. *L. m. schmidti*														100.00

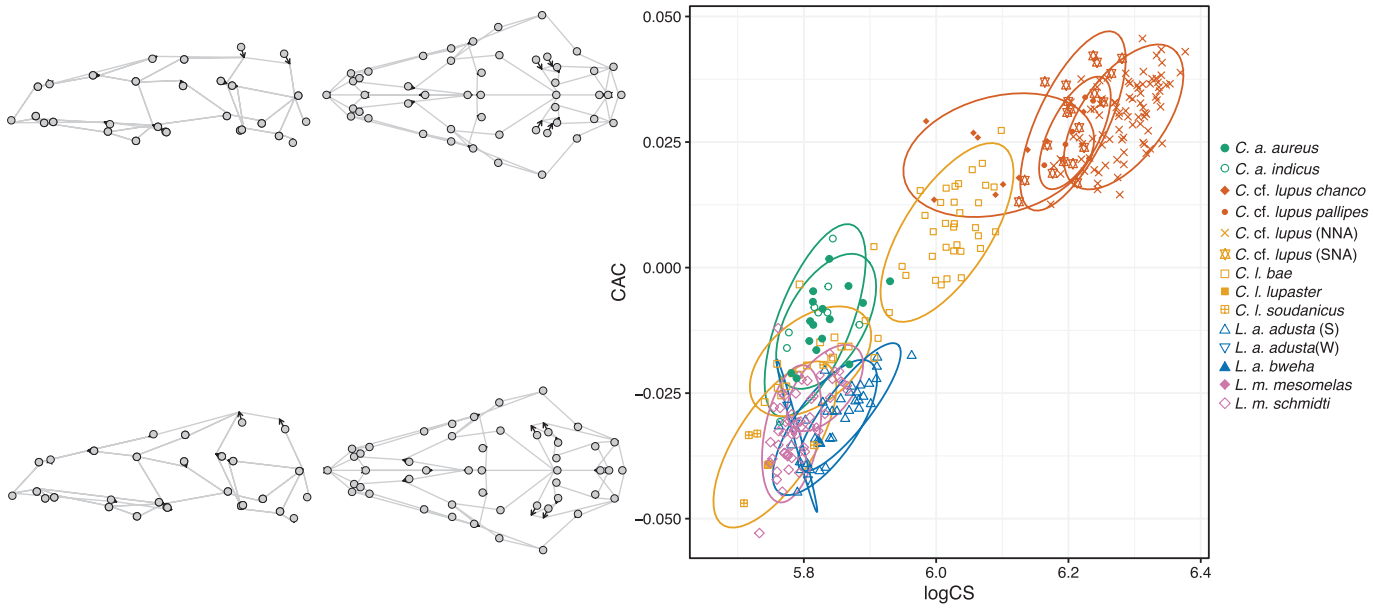

Fig. 6.—Relationship between the common allometric component (CAC) of *Canis* and *Lupulella* subspecies and size (logCS). Configurations represent shape changes associated with size differences on both lateral and dorsal views.

is further reinforced by the fact that *C. l. soudanicus* forms a morphological continuum with members of the *L. adusta* species on the analysis of the common allometric component CAC (Fig. 6). Taken together, these results suggest that the divergence observed among *C. l. soudanicus* and *L. adusta* is no different than the one observed among other *L. adusta* populations, both in shape (Fig. 4) and in size (Fig. 6). Thus, the most parsimonious explanation is that *C. l. soudanicus* might be a synonym of *L. adusta* instead of being part of the golden wolf complex.

The remaining two subspecies, *C. l. bea* and *C. l. lupaster*, refers to the small and large morphs described for the golden wolf complex (Fig. 7). While the first subspecies can be classified as having a generalized jackal morphology, clustering together with species such as *L. mesomelas* and *C. aureus* (Figs. 5 and 6), the second occupies an intermediate position on the morphospace between jackal-like forms and wolf-like forms, implying an intermediate morphology (Bertè 2017). Although both subspecies were morphometrically cohesive (i.e., showed high correct classification rates on the cross-validation analysis), some small overlap was observed between them. While we cannot rule out the possibility that different morphs of *C. lupaster* coexist at one locality (Gaubert et al. 2012), it is more likely that slight differences in allometric scaling might be at fault, as misclassified individuals were small in comparison to the remaining members of their subspecies. This fact could also explain the overlap of *C.* cf. *l. chanco* with *C. lupaster*, as the misclassified specimen had a juvenile-like morphology, despite fitting our criteria for adulthood. The CAC analysis is consistent with this interpretation, as allometric scaling can make younger (or smaller) individuals appear more similar to individuals from other taxa (Fig. 6). The overlap between *C. aureus*

with *C. l. bae*, on the other hand, cannot be readily explained in this way and could be evidence of the general morphological similarity between both taxa. In any regard, the identification of two discrete morphs of African golden wolves can be considered evidence for the existence of two species under the same name (Bertè 2017).

For canids, there is evidence showing that intraspecific allometry matches evolutionary allometry (Wayne 1986; Machado, pers. obs.), a phenomenon that could lead to taxonomic confusion (e.g., Prevosti et al 2013; Chemisquy et al. 2019). Large individuals of one species could be misclassified as belonging to a different taxon, even though they are not. In the case of the taxa investigated here, however, allometric scaling appears to be insufficient to explain all variation among taxa (Table 2). While LD1 (or PC1; data not shown) scores were greatly correlated with CAC scores, shape changes along both directions were not entirely aligned (Figs. 4 and 6; vector correlation = 0.551). This might seem paradoxical but, if size and shape are coevolving, this association is not necessarily being driven by ontogenetic constraints (Machado et al. 2018). Canidae is thought to be more evolutionarily flexible in terms of shape than other Carnivora, while at the same time possessing an increased allometric scaling on facial traits (Machado et al. 2018, 2019). Given that size can itself change as a response to dietary demands, size may be coevolving with other shape features not related to allometric scaling, thus producing an association between these aspects of morphology. This, however, is in contrast with a broad-scale analysis that showed that the skull evolution of Canidae is heavily influenced by ontogenetic constraints (Wayne 1986; Machado, pers. obs.). While differences between studies could be due to different morphometric methodologies (Euclidian distances versus geometric morphometrics; Machado et al. 2019), the misalignment of intraspecific and interspecific allometry could be restricted to the groups analyzed here. African species are under intense competition between taxa (Van Valkenburgh and Wayne 1994), a fact that could help them to overcome intraspecific constraints. If that is the case, broad-scale analyses might overlook phylogenetically restricted processes that could have shaped the morphological diversity in African and Asian taxa.

Explaining these morphological patterns in light of current knowledge of the genetics of the group can be daunting. Broad-scale mitochondrial genome studies have consistently shown that there is little genetic differentiation among *C. lupaster* populations (Gaubert et al. 2012; Koepfli et al. 2015; Urios et al. 2015; Viranta et al. 2017; Gopalakrishnan et al. 2018; Saleh et al. 2018). Nuclear data, both genomic (Gopalakrishnan et al. 2018) and microsatellite (Koepfli et al. 2015), have shown that there is a broad division among western and eastern populations of *C. lupaster.* Even though our sample does not contain western populations, Bertè (2017)'s craniometric analysis of *C. lupaster* specimens found throughout the continent showed that the main difference was between a larger and more robust morph from Egypt and Libya, referred to as *C. lupaster,* and a smaller, more gracile morph from Eritrea, Somalia, Tunisia, Algeria, and Libya, referred to as *C. anthus* . Thus, there seems to be a conflict between different levels of evidence, where mitochondrial data fail to identify differences between putative populations, and nuclear and morphological evidence points to the existence of distinct groups that are, in turn, incompatible. One possibility that cannot be ruled out is the role of hybridization

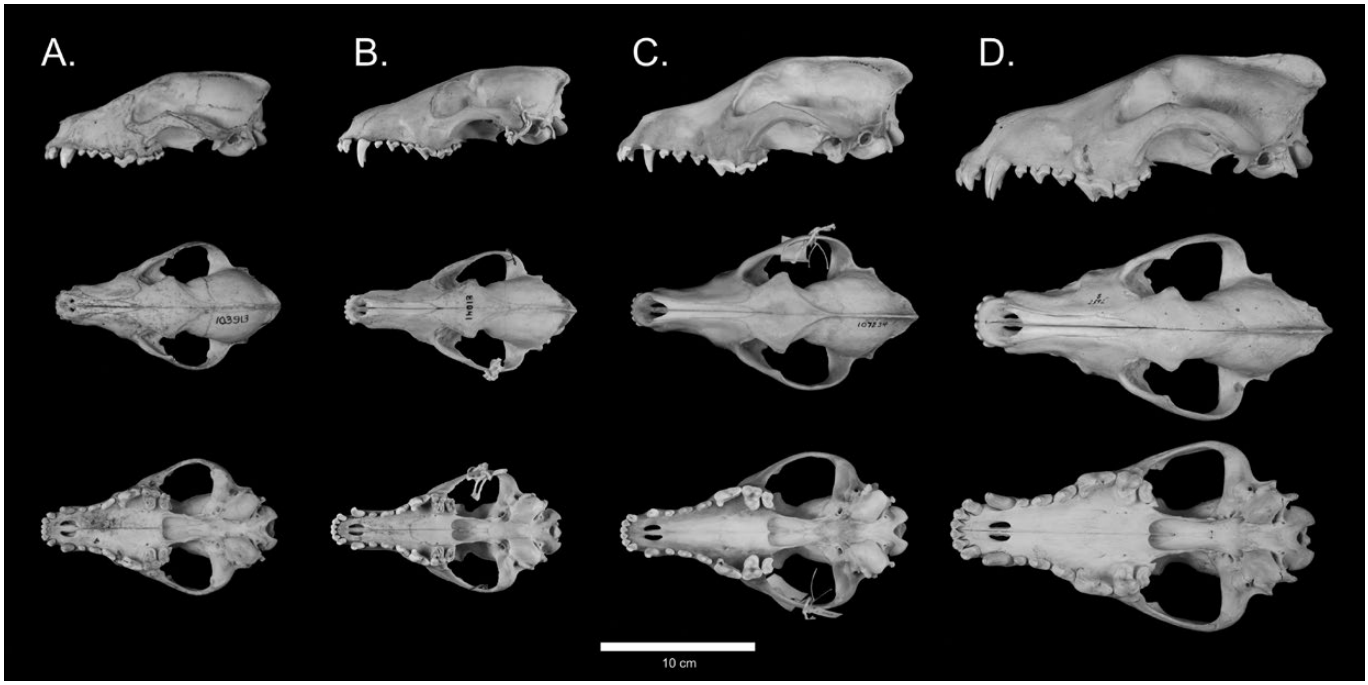

Fig. 7.—Comparison of the skull form in lateral, dorsal, and ventral views between "golden wolf" (*Canis aureus*) morphotypes with golden jackals (*C. lupaster*) and gray wolves (*C.* cf. *lupus*). (A) *Canis aureus* (FMNH 103913; Female). (B) Small morph of *C. lupaster* (AMNH 81041; Male). (C) Large morph of *C. lupaster* (FMNH 107234; Female). (D) *C.* cf. *lupus* (FMNH 7657; Female).

in generating morphological variance in specific populations. Gopalakrishnan et al. (2018) have shown that not only *C. lupaster* originates as a hybrid species, but that different populations went through further hybridization with different canid species (*C. simensis* in the east and *C.* cf. *lupus* in the northwest). Furthermore, their work shows the presence of a hybrid individual from the Sinai Peninsula possessing a mitochondrial genome compatible with that of the remaining African populations of *C. lupaster*, but with a nuclear genome associated with the gray wolf complex (Gopalakrishnan et al. 2018). It is not clear if this molecular composition is restricted to this single individual but, if not, that could help to explain why *C. l. lupaster* has an intermediate morphology between jackals and wolves (Figs. 5 and 6).

Lastly, our analysis also pointed out that *L. mesomelas* subspecies had almost no morphometric overlap (Fig. 4B). Recent mitochondrial studies have shown that there is a deep split between the southern *L. m. mesomelas* and the eastern *L. m. schmidti*, suggesting that these populations might represent different species (Atickem et al. 2017). While both populations are morphologically distinct (Supplementary Data SD4), canids have an increased capacity for evolutionary response on facial traits (Machado et al. 2018, 2019), making it difficult to rule out the action of differential selective pressure led by differences in feeding ecology of isolated populations. Furthermore, *L. adusta* also possesses an ancient split between western and eastern populations, a fact that is not reflected in our analysis, as all *L. adusta* populations greatly overlapped. Therefore, the actual taxonomic status of these distinct *L. mesomelas* populations is unclear, and if the morphological divergence between groups is representative of species divergence.

Taken together, our results raise the need for a taxonomic revision of various African canids, and the need to integrate diverse levels of evidence (e.g., Helgen et al. 2013). Inclusion of other African nominal forms, such as *algirensis* Wagner, 1841 or *riparius* Hemprich and Ehrenberg, 1833, both included within the synonymy of *lupaster* s.l., is much needed. The reassessment of type materials or topotypes is mandatory, and if they do not exist, evaluate the need to designate neotypes, to tie available names with defined morphologies and their corresponding molecular lineages.

Acknowledgments

For access to specimens under their care and other assistance during museum visits, we are grateful to M. de Vivo, J. Gualda, J. Oliveira, L. Flamarion, S. M. Vaz, E. Lacey, C. Conroy, N. B. Simmons, N. Duncan, E. Westwig, A. Marcato, E. Hoeger, K. Helgen, D. Lunde, E. Langan, J. Ososky, B. Patterson, B. Stanley, H. Hoekstra, J. Chupasko, T. Daeschler, and N. Gilmore. This article was supported by scholarships and grants from Fundação de Amparo à Pesquisa do Estado de São Paulo (2011/21674-4, 2013/22042–7), Santander and NSF (DEB 1350474 to L. Revell). We thank J. Esselstyn, E. Heske, and two anonymous reviewers for their inputs and comments, and M. C. Luna for proof-reading of the manuscript.

Supplementary Data

Supplementary Data SD1.—Bonferroni corrected *P*-values for the pairwise *t*-test between within-species disparities as measured through Mahalanobis distance.

Supplementary Data SD2.—Bonferroni corrected *P*-values for the pairwise *t*-test between within-subspecies disparities as measured through Mahalanobis distance.

Supplementary Data SD3.—Comparison of the skull in lateral, dorsal, and ventral views between the side-striped jackal (*Lupulella adusta*) and the Sudanese "golden wolf." (A) *L. adusta bweha* (FMNH 18948; sex indeterminate). (B) *Canis lupaster soudanicus* (USNM 318095; Female).

Supplementary Data SD4.—Comparison of the skull in lateral, dorsal, and ventral views between black-backed jackal (*Lupulella mesomelas*) subspecies. (A) *L. m. mesomelas* (AMNH 80652, Male); (B) *L. m. schimidti* (AMNH 27736, Female).

Literature Cited

Adams, D. C., M. L. Collyer, and A. Kaliontzopoulou. 2019. Geomorph: Software for geometric morphometric analyses. R package version 3.1.0. https://cran.r-project.org/package=geomorph. Accessed 25 March 2019.

Anderson, M. 2001. A new method for non-parametric multivariate analysis of variance. Austral Ecology 26:32–46.

Atickem, A., N. C. Stenseth, M. Drouilly, S. Bock, C. Roos, and D. Zinner. 2017. Deep divergence among mitochondrial lineages in African jackals. Zoologica Scripta 79:161–168.

Bertè, D. F. 2017. Remarks on the skull morphology of *Canis lupaster* Hemprich and Herenberg, 1832 from the collection of the natural history museum "G. Doria" of Genoa, Italy. Natural History Sciences 4:19–11.

Campbell, N., and W. Atchley. 1981. The geometry of canonical variate analysis. Systematic Zoology 30:268–280.

Chemisquy, M. A., et al. 2019. How many species of grey foxes (Canidae, Carnivora) are there in southern South America? Mastozoología Neotropical 26: 81–97.

Chetri, M., Y. Jhala, S. R. Jnawali, N. Subedi, M. Dhakal, and B. Yumnam. 2016. Ancient himalayan wolf (Canis lupus chanco) lineage in upper mustang of the annapurna conservation area, Nepal. ZooKeys 582:143–156.

De Beaux, O. 1923. Mammiferi della Somalia italiana. Raccolta del Maggiore Vittorio Tedesco Zammarano nel Museo Civico di Milano. Atti Societa Italiana di Scienze Naturali Milano 62: 247–316.

Diersing, V. E., and D.E. Wilson. 2017. Systematic status of the rabbits *Sylvilagus brasiliensis* and *S. sanctaemartae* from northwestern South America with comparisons to Central American populations. Journal of Mammalogy 98:1641–1656.

Ferguson, W. W. 1981. The systematic position of *Canis aureus lupaster* (Carnivora: Canidae) and the occurrence of *Canis lupus* in North Africa, Egypt and Sinai. Mammalia 4:459–465.

Gaisford, T. 1824. Notes on Herodotus. Oxford University. Oxford, United Kingdom.

Gaubert, P., and A. Antunes. 2005. Assessing the taxonomic status of the Palawan pangolin *Manis culionensis* (Pholidota)

using discrete morphological characters. Journal of Mammalogy 86:1068–1074.

Gaubert, P., et al. 2012. Reviving the African wolf *Canis lupus lupaster* in North and West Africa: a mitochondrial lineage ranging more than 6,000 km wide. PLoS One 7:e42740.

Gopalakrishnan, S., et al. 2018. Interspecific gene flow shaped the evolution of the Genus *Canis*. Current Biology 28:3441–3449.e5.

Helgen, K. M., et al. 2013. Taxonomic revision of the olingos (*Bassaricyon*), with description of a new species, the Olinguito. ZooKeys 324:1–83.

Hemprich, F. G., and C. G. Ehrenberg. 1831. Symbolae physicae, seu icones et descriptiones mammalium. Berolini ex Officina Academica. Berlin, Germany.

Heppenheimer, E., et al. 2018. Population genomic analysis of North American Eastern Wolves (*Canis lycaon*) supports their conservation priority status. Genes 9:606–18.

Hohenlohe, P. A., et al. 2017. Comment on "Whole-genome sequence analysis shows two endemic species of North American wolf are admixtures of the coyote and gray wolf." Science Advances 3:e1602250.

Khosravi, R., H. R. Rezaei, and M. Kaboli. 2013. Detecting hybridization between Iranian wild wolf (*Canis lupus pallipes*) and free-ranging domestic dog (*Canis familiaris*) by analysis of microsatellite markers. Zoological Science 30:27–35.

Klingenberg, C. P., M. Barluenga, and A. Meyer. 2002. Shape analysis of symmetric structures: quantifying variation among individuals and asymmetry. Evolution 56:1909–1920.

Koepfli, K. P., et al. 2015. Genome-wide evidence reveals that African and Eurasian golden jackals are distinct species. Current Biology 25:2158–2165.

Machado, F. A., and E. Hingst-Zaher. 2009. Investigating South American biogeographic history using patterns of skull shape variation on *Cerdocyon thous* (Mammalia: Canidae). Biological Journal of the Linnean Society 98:77–84.

Machado, F. A., T. M. G. Zahn, and G. Marroig. 2018. Evolution of morphological integration in the skull of Carnivora (Mammalia): changes in Canidae lead to increased evolutionary potential of facial traits. Evolution 72:1399–1419.

Machado, F. A., A. Hubbe, D. Melo, A. Porto, and G. Marroig. 2019. Measuring the magnitude of morphological integration: the effect of differences in morphometric representations and the inclusion of size. Evolution 33:402–11.

Marques, D. A., J. I. Meier, and O. Seehausen. 2019. A combinatorial view on speciation and adaptive radiation. Trends in Ecology & Evolution 34:531–544.

Mayr, E. 1942. Systematics and the origin of species. Columbia University Press. New York.

Mech, L. D. 1974. Canis lupus. Mammalian Species 37:1–6.

Miranda, F. R., D. M. Casali, F. A. Perini, F. A. Machado, and F. R. Santos. 2017. Taxonomic review of the genus Cyclopes Gray, 1821 (Xenarthra: Pilosa), with the revalidation and description of new species. Zoological Journal of the Linnean Society 183:687–721.

Mitteroecker, P., and F. Bookstein. 2011. Linear discrimination, ordination, and the visualization of selection gradients in modern morphometrics. Evolutionary Biology 38:100–114.

Mitteroecker, P., P. Gunz, M. Bernhard, K. Schaefer, and F. L. Bookstein. 2004. Comparison of cranial ontogenetic trajectories among great apes and humans. Journal of Human Evolution 46:679–697.

Moehlman, P. D., and V. Hayssen. 2018. *Canis aureus* (Carnivore: Canidae). Mammalian Species 50:14–25.

Morey, D. F. 1992. Size, shape and development in the evolution of the domestic dog. Journal of Archaeological Science 19: 181–204.

Pilot, M., et al. 2018. Widespread, long-term admixture between grey wolves and domestic dogs across Eurasia and its implications for the conservation status of hybrids. Evolutionary Applications 11:662–680.

Prevosti, F. J., V. Segura, and G. H. Cassini. 2013. Revision of the systematic status of patagonian and pampean gray foxes (Canidae: *Lycalopex griseus* and *L. gymnocercus*) using 3D geometric morphometrics. Mastozoología Neotropical 20: 289–300.

Pocock, R. I. 1935. The races of *Canis lupus*. Proceedings of the Zoological Society of London 105:647–686.

Rohlf, F., and D. Slice. 1990. Extensions of the procrustes method for the optimal superimposition of landmarks. Systematic Zoology 39:40–59.

Rueness, E. K., et al. 2011. The cryptic African wolf: Canis aureus lupaster is not a golden jackal and is not endemic to Egypt. PLoS One 6:e16385.

Saleh, M. A., and M. I. Basuony. 2014. Mammals of the genus canis Linnaeus, 1758 (Canidae, Carnivora) in Egypt. Egyptian Journal of Zoology 62:49–92.

Saleh, M., M. Younes, M. Sarhan, and F. Abdel-Hamid. 2018. Melanism and coat colour polymorphism in the Egyptian Wolf *Canis lupaster* Hemprich & Ehrenberg (Carnivora: Canidae) from Egypt. Zoology in the Middle East 64:195–206.

Schlager, S. 2017. Morpho and Rvcg- shape analysis in R: R-packages for geometric morphometrics, shape analysis and surface manipulations. Pp. 217–256 in Statistical shape and deformation analysis (G. Zheng, S. Li and G. Szekely, eds.). Academic Press. Cambridge, Massachusetts.

Schönemann, P. H. 1966. A generalized solution of the orthogonal Procrustes problem. Psychometrika 31:1–10.

Setzer, H. W. 1956. Mammals of the Anglo-Egyptian sudan. Proceedings of the United States National Museum 106:447–587.

Sillero-Zubiri, C., M. Hoffmann, and D. W. Macdonald. 2004. Canids: foxes, wolves, jackals, and dogs: status survey and conservation action plan. IUCN. Gland, Switzerland.

Slice, D. E. 2001. Landmark coordinates aligned by procrustes analysis do not lie in Kendall's shape space. Systematic Biology 50:141–149.

Urios, V., M. P. Donat-Torres, and C. Ramírez. 2015. El análisis del genoma mitocondrial del cánido estudiado en Marruecos manifiesta que no es ni lobo (*Canis lupus*) ni chacal euroasiático (*Canis aureus*). AltoterO 3:1–15.

Van Valkenburgh, B., and R. K. Wayne. 1994. Shape divergence associated with size convergence in sympatric East African Jackals. Ecology(Durham) 75:1567–1581.

Viranta, S., A. Atickem, L. Werdelin, and N. C. Stenseth. 2017. Rediscovering a forgotten canid species. BMC Zoology 2:1–9.

vonHoldt, B. M., et al. 2016. Whole-genome sequence analysis shows that two endemic species of North American wolf are admixtures of the coyote and gray wolf. Science Advances 2:e1501714.

Voss, R. S., K. M. Helgen, and S. A. Jansa. 2014. Extraordinary claims require extraordinary evidence: a comment on Cozzuol *et al*. (2013). Journal of Mammalogy 95:893–898.

Walton, L. R., and D. O. Joly. 2003. Canis mesomelas. Mammalian Species 715:1–9.

Way, J. G. 2013. Taxonomic implications of morphological and genetic differences in northeastern coyotes (coywolves)(*Canis latrans* × *C. lycaon*), western coyotes (*C. latrans*), and eastern wolves (*C. lycaon* or *C. lupus lycaon*). The Canadian Field-Naturalist 127:1–16.

Wayne, R. K. 1986. Cranial morphology of domestic and wild canids: the influence of development on morphological change. Evolution 40:243–261.

Zrzavý, J., P. Duda, J. Robovský, I. Okřinová, and V. P. Ričánková. 2018. Phylogeny of the Caninae (Carnivora): combining morphology, behaviour, genes and fossils. Zoologica Scripta 47:373–389.

Submitted 11 April 2019. Accepted 21 December 2019.

Associate Editor was Jacob Esselstyn.

Appendix I

Specimens analyzed

Lupulella adusta adusta (S)- AMNH 216344♂, AMNH 116335♀, AMNH 160990♀, AMNH 116333♂, AMNH 160989♀, AMNH 160997♀, AMNH 116334♀, FMNH 83641♀, FMNH 38184♂, FMNH 38185♀, FMNH 95999♀, FMNH 95933♂, MCZ 44289♀, MCZ 44290♂, MVZ 118415♂, USNM 61759♂, USNM 470131♀, USNM 399437♂; *L. a. adustus* (W)- FMNH 42121♂, MVZ 149525♂, MVZ 149524♂; *L. a. bweha*- AMNH 52049♂, AMNH 81039♀, AMNH 114259♀, AMNH 54212♀, AMNH 27725♀, AMNH 179136♂, AMNH 52057♂, FMNH 27248♀, FMNH 32936♂, FMNH 18939♂, FMNH 18948♂, FMNH 73036♀, FMNH 73037♀, MCZ 37939♀, MCZ 45890♀, MVZ 155564♂, USNM 182343♂, USNM 181488♀, USNM 182348♂, USNM 162137♂.

Lupulella mesomelas mesomelas- MVZ 33389♂, AMNH 233009♂, AMNH 80652♂, AMNH 233010Ø, AMNH 169095♀, MVZ 117811♀, MVZ 117810♀, MVZ 117808Ø, MVZ 118420♀, MVZ 118419♀, MVZ 117809♂, MVZ 117807♂, MVZ 117802♂, MVZ 118416♂, AMNH 169447♀; *L. m. schmidti*- MVZ 173765♀, AMNH 27736♀, AMNH 27731♂, AMNH 34731♂, AMNH 34732♂, AMNH 187716♀, AMNH 114267♂, AMNH 187727♀, AMNH 54208♀, AMNH 54211♂, AMNH 54213♂, AMNH 54206♂, AMNH 179139♂, AMNH 179137♂, AMNH 179140♀, AMNH 54209♂, AMNH 114177♂, AMNH 82398♀, AMNH 114179♀, AMNH 114180♀, AMNH 205145♂, AMNH 205146♀, AMNH 187715♂, AMNH 187711♀, AMNH 114228♂, AMNH 187713♀, AMNH 187712♂, MVZ 165153♀, MVZ 165156♂, MVZ 165142♂, MVZ 165141♂, MVZ 165152♀, MVZ 1651157♀, MVZ 165154♀, MVZ 165158♂, MVZ 165150♀, MVZ 165140♀, MVZ 165151♀, MVZ 165145♂, MVZ 165143♂, MVZ 165147♂, MVZ 165146♂, MVZ 99398Ø

Canis lupaster bea- AMNH 81041♂, AMNH 81040♀, AMNH 27726♀, AMNH 27732♀, AMNH 27735♀, AMNH 27733♀, AMNH 27739♀, AMNH 187714♂, AMNH 114175♂, FMNH 27155♂, FMNH 27147♂, FMNH 27152♀, FMNH 27156♂, FMNH 27150♂, MVZ 173749♀, FMNH 27158♀; *C. l. lupaster*- FMNH 140116♂, FMNH 107340♂, FMNH 107231♀, FMNH 107227♀, FMNH 107234♀, FMNH 107232♂, FMNH 107337♀, FMNH 107230♂, FMNH 107338♀, FMNH 107336♂, FMNH 140115♀, FMNH 121349♀, FMNH 107228♂, FMNH 107229♀, FMNH 140119♂, FMNH 107236♂, FMNH 140118♀, FMNH 105807♂, FMNH 140117♂, FMNH 105742♀, FMNH 106723♂, FMNH 106722♂, FMNH 105740♀, FMNH 105744♂, FMNH 106724♂, FMNH 105741♂, FMNH 105743♀, FMNH 108364♂, FMNH 140124♂, FMNH 107223♂, FMNH 75647♂, FMNH 98921♀, FMNH 89967♂, FMNH 89966♀, FMNH 107226♀, FMNH 140122Ø, FMNH 96233♂; *C. l. sudanicus*- USNM 350071♂, USNM 318095♀, USNM 299841♀, USNM 350072♀, USNM 342087♀, USNM 342085♂, USNM 342088♀.

Canis aureus aureus- AMNH 88708♀, AMNH 88709♂, AMNH 88712♂, FMNH 103912♀, FMNH 103913♀, FMNH 103914♀, FMNH 103920♀, FMNH 103910♀, FMNH 103916♀, FMNH 103909♂, FMNH 112371♂, FMNH 112364♂, FMNH 57264♂, FMNH 97773♀, FMNH 112372♂, MZUSP 2568♀; *C. a. indicus*- AMNH 54516♂, AMNH 54515♀, FMNH 29757♀, FMNH 29790♂, FMNH 29756♀, FMNH 35672♂, FMNH 83076♂, FMNH 83078♀, FMNH 91242♀;

Canis cf.*lupus chanco*- ANSP 17498♂, ANSP 17497♂, ANSP 17496Ø, MCZ 24870Ø, MCZ 24873♂, USNM 172654♀, USNM 198458♀, USNM 19846Ø, USNM 172655♀, USNM 198457♂; *C.* cf.*lupus pallipes*- FMNH 44469♂, FMNH 44467♀, FMNH 44471♀, FMNH 44470♀, FMNH 46079Ø, FMNH 99417Ø; *C.* cf.*lupus* spp(NNA)- FMNH 7657♀, FMNH 128794♂, FMNH 138790♂, FMNH 138795♀, FMNH 138773♂, FMNH 138783♀, FMNH 138774♀, FMNH 138772♂, FMNH 138779♀, FMNH 138782♀, FMNH 138781♀, FMNH 13778♂, FMNH 138784♀, FMNH 128780♂, FMNH 138785♀, FMNH 138792♂, FMNH 138787♂, FMNH 138793♂, FMNH 138788♀, FMNH 138789♀, FMNH 138791♀, FMNH 138786♂, FMNH 138797♂, FMNH 150997♀, FMNH 72961♂, FMNH 72962♀, MCZ 39658♀, MCZ 50508♂, MNRJ 32366♂, MVZ 8321♂, MVZ 59682♀, MVZ 5681♂, MVZ 57343♂, MVZ 76253♀, MVZ 47276♀, MVZ 472777♀, MVZ 31042♀, MVZ 31043♂, MVZ 12454♂, MVZ 12455♂, MVZ 12457♂, MVZ 28003♀, MVZ 28004♀, MVZ 28001♂, MVZ 28002♂, MVZ 29772♀, MVZ 30515♂, MVZ 31234♂, MVZ 184046♀, MVZ 159321♀, MVZ 95177♂, MVZ 99746♀, MVZ 4777♂, MVZ 44166♂, MVZ 4776♂, MVZ 184047♀, MVZ 984♂, MVZ 77345♂, MVZ 123980♀, MVZ 77346♂, MVZ 77742♂, MVZ 119835♀, MVZ 88226♀, MVZ 88225♂, MVZ 123978♂, MVZ 119833♂, MVZ 84200♀, MVZ 119834♀, MVZ 119836♂, MVZ 119832♀, MVZ 125603♀, MVZ 123999♂, MVZ 122232♀, MVZ 123981♂, MVZ 123983♀, MVZ 125604♂, MVZ 125607♂, MVZ 122234♂, MVZ 125606♀, MVZ 122233♀, MVZ 122230♂, MVZ 122231♂, MVZ 128114♂, MVZ 224392♂, MVZ 184048♂, MZUSP 2569♂; *C.* cf.*lupus* spp(SNA)- FMNH 7619♀, FMNH 21750♀, FMNH 21751♂, MVZ 109615♂, MVZ 32422♂, MVZ 35380♀, MVZ 129254♂, MVZ 74827♀, MVZ 138927♂, MVZ 74828♂, MVZ 31973-B♂, MVZ 109614♂, MVZ 74829♀, MVZ 109617♂, MVZ 35387♂, MVZ 35381♂, MVZ 34228♂, MVZ 76254♂, MVZ 171944♀, MVZ 33389♂.